

## Performance analysis of a multifrequency radiometer for predicting atmospheric propagation parameters

G. Schiavon and D. Solimini

Dipartimento di Ingegneria Elettronica, Università Tor Vergata, Roma, Italy

E. R. Westwater

National Oceanic and Atmospheric Administration, Environmental Research Laboratory Wave Propagation Laboratory, Boulder, Colorado

(Received April 7, 1992; revised July 28, 1992; accepted August 3, 1992.)

This study concerns the predicted performance of multifrequency ground-based radiometers in estimating atmospheric moisture and the corresponding attenuation and wet path delay on an Earth-space path. The analysis of the performance is based on a numerical simulation using possible combinations of radiometric channels at 10 microwave frequencies below 100 GHz. We first discuss the accuracy of retrievals of both integrated atmospheric vapor and cloud liquid from noisy radiometric measurements carried out at two frequencies and investigate the improvement attainable by using more than two radiometric channels. Then we focus on the problem of predicting attenuation and wet path delay at several frequencies in the millimeter wave range for a vertical Earth-space path from radiometric data. Examples of possible combinations of two and three frequencies are presented, ranked according to their capability, first in retrieving vapor and liquid, then in predicting attenuation and wet path delay for two different climatologies.

### 1. INTRODUCTION

The behavior of a radio path through a nonscattering atmosphere is characterized by two principal quantities, that is, cumulative path attenuation  $A$ :

$$A = (4.34) \int_0^R \alpha(s) ds \quad \text{dB} \quad (1)$$

and path delay (or excess propagation length)  $D$ :

$$D = (0.1) \int_0^R \Re[N(s)] ds \quad \text{cm} \quad (2)$$

where  $\alpha(s)$  (per kilometer) is the absorption coefficient,  $\Re[N(s)]$  (in ppm  $\equiv 10^{-6}$ ) is the real part of the complex refractivity and  $R$  (in kilometers) the total atmospheric path length. Both  $A$  and  $D$  are evaluated over line integrals that are evaluated on the refracted ray path whose differential path length is  $ds$  (in kilometers). These propagation parameters are functions of the physical state of the air, which is described by several meteorological variables,

including temperature  $T$ , water vapor partial pressure  $e$ , and liquid water density  $\rho_w$ . At frequencies beyond 10 GHz, rain severely limits atmospheric propagation. However, we consider here only the effect of nonprecipitating clouds. Indeed, with the expanded use of frequencies above 20 GHz, low fade margin systems become increasingly important, and for these systems, both water vapor and cloud liquid are key factors in determining the propagation characteristics.

For a nonscattering atmosphere in local thermodynamic equilibrium, the brightness temperature at ground is related to the absorptive properties of the medium by

$$T_B = \int_0^\infty T(s)\alpha(s)e^{-\int_0^s \alpha(s') ds'} ds + T_{\text{cos}} e^{-\int_0^\infty \alpha(s) ds}. \quad (3)$$

In (3),  $T(s)$  (in degrees Kelvin) is the atmospheric physical temperature at the spatial coordinate  $s$ , and  $T_{\text{cos}}$  (also in degrees Kelvin) is the brightness temperature contributed by extraterrestrial sources (cosmic background). For nonprecipitating conditions in the troposphere,  $T_B$  depends essentially on frequency and viewing direction and is unpolarized.  $T_B$  data contain information on the state of the atmosphere, so that the retrieval of the spatial

Copyright 1993 by the American Geophysical Union.

Paper number 92RS02457.  
0048-6604/93/92RS-02457\$8.00

distributions of temperature and of the absorbing/emitting gases or water particles is, in principle, feasible from radiometric measurements. If the absorption is sufficiently weak ( $\leq 12$  dB), the atmospheric opacity can be derived from brightness temperature measurements. The accuracy of the opacity determination depends on the accuracy to which the effective medium temperature can be estimated. Furthermore, the total amount of water vapor  $V$  in the air column sensed by the radiometer antenna and the corresponding total integrated liquid water  $L$  can be obtained from the opacity measured at two frequencies for which the effects of the two phases differ substantially. In practice, because of spatial inhomogeneities, especially during cloudy conditions, equal antenna beam widths are required at both frequencies for accurate determination of  $V$  and  $L$ .

To this end, dual-channel radiometers have been operated for several years to measure  $V$  and  $L$  [Askne and Westwater, 1986; Elgered et al., 1982; Hogg et al., 1983]. Frequencies around 20 GHz and 31 GHz are used, since the lower one, on one shoulder of the water vapor absorption line, yields measurements that are nearly independent of the height distribution of water vapor, while the upper is particularly sensitive to the liquid. The retrievals have been generally carried out by the linear statistical method [Westwater and Strand, 1968]. The accuracies of retrievals from dual-channel radiometric data, which are reported to be typically 1.0 to 1.5 mm for vapor and better than 20% for liquid, are satisfactory for several applications [Snider, 1988]. However, it should be mentioned that the experimental data base is not wide enough to include the various relevant climatic conditions which can be encountered around the world. In addition, since the routinely launched radiosondes do not measure liquid water, atmospheric truth to verify the accuracy of liquid retrievals is difficult to obtain. In addition, the errors of liquid and, in particular, of vapor retrievals appear to increase dramatically with increasing integrated amounts of liquid [Westwater and Guiraud, 1980]. Indeed, a major source of error seems to be the dependence of the absorption coefficient of liquid on temperature. Westwater and Guiraud [1980] have examined the influence of cloud temperature error on the accuracy of vapor retrieval and found that by using long-term average temperature data only, errors on the order of 50% can be expected, even for a moderately dense cloud

bearing 5 mm of liquid. Although the use of the adaptive statistical inversion [Westwater and Guiraud, 1980] can reduce the retrieval error, when the integrated cloud liquid increases beyond  $\sim 6$  mm, the accuracy rapidly degrades if the actual cloud temperature is not taken into account. A possible way of overcoming this difficulty is the use of radiometers with more than two channels, so that the thermal state of the atmosphere can also be retrieved from the multifrequency data. Ideally, a temperature and humidity profiling system should yield a good performance. However, a simpler instrument could be devised that would have the potential of retrieving the key atmospheric parameters without substantial loss of accuracy with respect to the ideal system in a variety of climatic conditions.

With this purpose in mind, we have carried out a numerical simulation to analyze the accuracy of retrievals of integrated atmospheric vapor and cloud liquid from dual frequency noisy radiometric measurements and the possible improvement of accuracy attainable by using an additional radiometric channel. Nevertheless, atmospheric vapor and liquid are not the only quantities that can be directly used in telecommunications [Brussaard, 1985] and space geodesy [Gary et al., 1985; Ware et al., 1985; Elgered et al., 1991], although the wet path delay depends essentially on vapor. Indeed, if a radiometric system has to provide data for satellite communication studies and/or for space geodesy applications, its optimal configuration should be determined with respect to the accuracy with which the relevant propagation parameters (i.e., attenuation and tropospheric electrical path delay) can be predicted from the radiometric data. To investigate the effects of different selections of the radiometric frequencies and of the number of channels, our numerical simulation has been extended to attain the ranking of different sets of frequencies with respect to the accuracy of predicting zenith attenuation  $A$  and wet path delay  $D$ . We used H. Liebe's Microwave Propagation Model (MPM) [Liebe, 1989] to evaluate  $A$  and  $D$  from the height profiles of meteorological variables. A statistical comparison between these values of  $A$  and  $D$  and those predicted from the radiometric data leads us to rank the combinations of radiometric frequencies with respect to their accuracy in zenith attenuation and wet path delay predictions.

Some of the questions addressed here were ex-

amined by *Grody* [1976] for satellite-based observations. For a space-based platform, he showed that, for a single frequency system, a frequency at 22.235 is optimum for water vapor and one around 40 GHz is optimum for liquid. He also investigated the effects of a second frequency, both with one and two frequencies fixed. However, because of the effects of a variable surface emissivity on satellite observations, optimum location of frequencies will in general be different from ground- and space-based platforms.

## 2. RETRIEVAL OF VAPOR AND LIQUID

Knowledge of the spatial distributions of temperature and absorbing constituents, as well as of the dependence of the absorption coefficient on temperature, pressure, and composition of the atmosphere, allows one to calculate brightness temperature at ground  $T_B(0)$  from meteorological profiles (direct problem). On the other hand,  $T_B(0)$  data contain information on the state of the atmosphere, so that the retrieval of the spatial distributions of temperature and of the absorbing/emitting gases or water particles is, in principle, feasible from suitable sets of radiometric measurements (inverse problem).

In the procedure commonly followed in retrieving water vapor and liquid water content of the atmosphere, an "optical" depth  $\tau(0, s)$ , given by

$$\tau(0, s) = \int_0^s \alpha(s') ds', \quad (4)$$

and a mean radiating temperature  $T_{mr}$ , given by

$$T_{mr} = \frac{\int_0^\infty T(s)\alpha(s)e^{-\tau(0, s)} ds}{1 - e^{-\tau(0, \infty)}}, \quad (5)$$

are defined, in order to transform (3) into

$$T_B(0) = T_{\cos} e^{-\tau(0, \infty)} + T_{mr}[1 - e^{-\tau(0, \infty)}]. \quad (6)$$

Solving (6) for  $\tau(0, \infty)$  yields

$$\tau(0, \infty) = -\ln \left( \frac{T_{mr} - T_B(0)}{T_{mr} - T_{\cos}} \right). \quad (7)$$

The total amount of water vapor  $V$  in the air column probed by the radiometer antenna and the corre-

sponding total integrated liquid water  $L$  are then obtained from the total atmospheric absorption, or opacity,  $\tau(0, \infty)$  measured at two frequencies at which the effect of the two phases differs substantially.

To assess the influence of different climatologies on retrieval accuracy, two widely different climatic conditions have been selected, that is, mid-latitude summer and subarctic winter. It is believed that, with the exception of some tropical conditions, a large majority of the climatologies of interest will fall within the range spanned by the two that have been considered.

Training and evaluation sets of atmospheric realizations were statistically generated starting from mid-latitude summer standard atmospheres [*McClatchey and D'Agati*, 1978]. Corresponding sets of brightness temperatures at 10 frequencies in the range 16–90 GHz have been computed for a ground-based zenith-looking radiometer by the MPM [*Liebe*, 1989]. Then various combinations of two and three brightness temperatures, corrupted by Gaussian noise of different rms amplitude, were used to retrieve the zenith-integrated amount of atmospheric water vapor and cloud liquid. Intermediate steps required first the derivation of  $\tau(0, \infty)$  from  $T_B(0)$  and then the subsequent application of statistical linear regression analysis. The retrieved values have been compared with the actual values as given by the atmospheric profiles and an rms accuracy has been evaluated for both vapor and liquid. The combinations of frequencies were then ranked in order of decreasing retrieval accuracy for vapor and liquid. Finally, the entire procedure was repeated for the subarctic winter atmosphere. To obtain statistically meaningful results, sets of at least 6,000 synthetic data were used in each simulation.

### 2.1. Atmospheric profile generation

Two statistically independent ensembles of atmospheric profiles were generated starting from the mid-latitude summer standard atmosphere. For temperature, at ground level a random fluctuation with a Gaussian distribution has been superimposed on its standard value. Random fluctuations were also added to the temperature values at different heights but with a  $\Gamma$  distribution [*Soong*, 1982]. These fluctuations were added to a projected adiabatic profile to avoid unphysical situations. Ground-

based thermal inversions with  $\Gamma$ -distributed thickness and strength were included too.

The profiles of water vapor have been constructed by adding random irregularities with a Gaussian distribution to the standard atmosphere profile. Liquid water simulating fog and/or clouds was generated whenever the relative humidity at a given height was larger than a selected threshold. Both the thickness of the fog layer and the base height of the clouds were  $\Gamma$ -distributed, and the same distribution controlled the statistical generation of cloud thickness. The liquid content of clouds has been assumed to be proportional to their thickness [Decker *et al.*, 1978]. A mixture of liquid and ice has been assumed below 0°C, while only ice is present below -30°C.

In total, one third of the profiles referred to clear skies, one third referred to fog conditions, and one third referred to cloudy conditions. The average integrated vapor for mid-latitude summer was 29.7 mm, with an rms standard deviation of 6.2 mm, and the corresponding quantities for total liquid were 0.65 and 0.11 mm. The same procedure was followed to generate the ensembles of profiles for the subarctic winter case, for which the average vapor was 5.4 mm with standard deviation of 3.3 mm and the average liquid 0.08 mm with 0.14 mm standard deviation.

Note that such a set of synthetic height profiles can be brought to approximate statistically an ensemble of profiles actually measured by radiosondes on a particular location, by suitably adjusting the various parameters that enter the profile generation, that is, mean values and variance of temperature and humidity at ground, mean and variance of integrated vapor and liquid, their distribution with height, percent of cloud cover, etc. Note that some of the parameters entering the profile generation are not measured by radiosondes.

## 2.2. Brightness temperatures

The synthetic realizations of atmospheric profiles for mid-latitude summer and for subarctic winter conditions were used as inputs to Liebe's MPM to obtain the brightness temperatures as would be measured by a ground-based microwave radiometer aiming at zenith. Ten frequencies, mainly lying in bands protected by radio frequency allocation, have been selected with the intention of assessing the potential of different combinations in atmospheric

TABLE 1. Means and Standard Deviations of Radiating Temperatures of the Ensembles of Atmospheric Profiles Used in the Simulation

$f$ , GHz	$T_{mr}$ , K			
	Midlatitude Summer		Subarctic Winter	
	Mean	Standard Deviation	Mean	Standard Deviation
16.0	281.0	5.1	247.5	7.1
20.6	283.1	4.7	250.7	7.7
22.2	281.8	4.0	251.2	7.6
23.9	283.4	4.6	250.9	7.7
31.6	281.7	5.0	247.9	7.0
36.0	280.9	4.8	247.4	6.9
50.0	277.6	3.8	245.6	6.4
54.0	283.2	3.1	250.1	6.3
58.0	292.5	3.2	257.7	6.4
90.0	285.6	4.7	250.7	7.4

parameter retrieval. Four frequencies were chosen in atmospheric windows, that is, 16.0, 31.6, 36.0, and 90.0 GHz; three frequencies close to the 22.235 GHz water vapor line, that is, 20.6, 22.2, and 23.8 GHz, and three frequencies on the lower frequency wing of the 60-GHz oxygen complex, that is, 50.0, 54.0, and 58.0 GHz.

Means and standard deviations of radiating temperatures, at these frequencies, of the ensembles of profiles used in the simulation are reported in Table 1. The behavior of the brightness temperatures at some of the mentioned frequencies as a function of the statistically generated total amount of atmospheric liquid is shown in Figure 1. As expected, the radiometric channels at 54 and 58 GHz appear to be substantially insensitive to the liquid (and to vapor also), whereas, as indicated by their weighting functions [Westwater *et al.*, 1990] (not shown here), they respond to temperature. On the other side, the 90-GHz channel is quite sensitive to liquid, but its response tends to saturate beyond 2 mm of liquid water. For this reason, it does not appear suitable for liquid retrieval in climatic conditions favorable to the development of thick and dense water clouds.

For profiles with ice clouds or, in general, with scarce atmospheric liquid, the 90-GHz channel is less subject to saturation and, in principle, can contribute effectively to the retrievals. The radiometric response for these kinds of situations in terms of brightness temperature versus vertically integrated liquid is shown in Figure 2 for some of the considered frequencies.

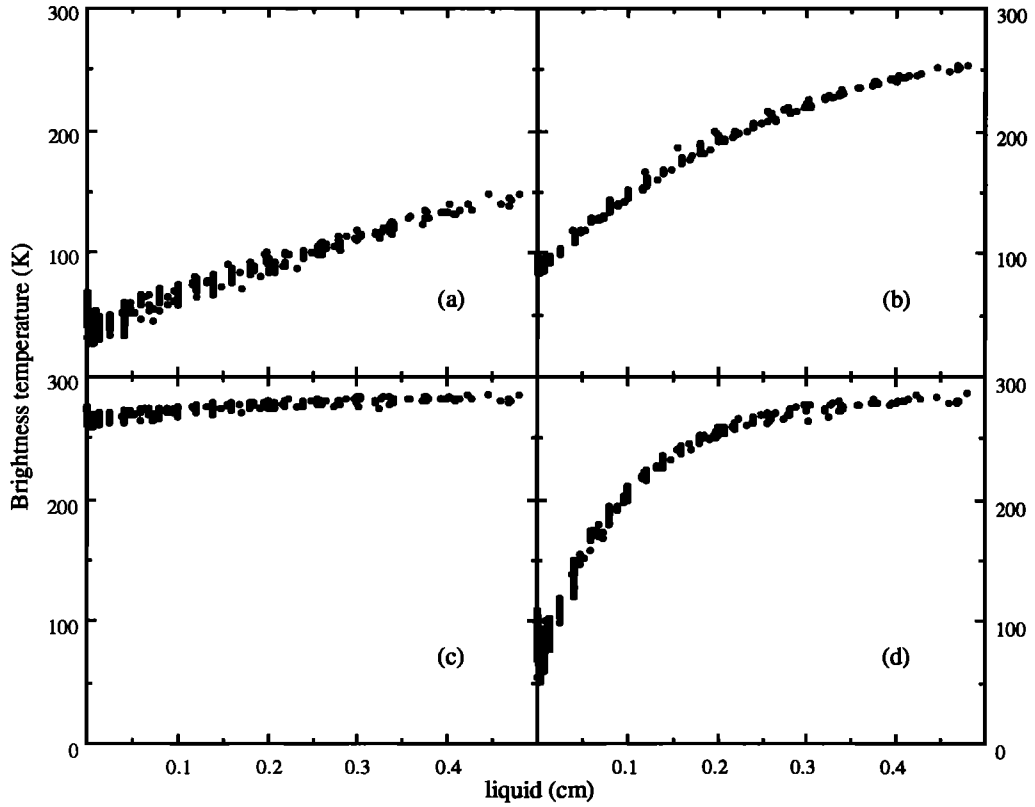


Fig. 1. Brightness temperature for zenith-looking radiometer at (a) 23.9, (b) 50.0, (c) 54.0, and (d) 90.0 GHz for mid-latitude summer conditions versus liquid water of clouds.

### 3. OPTIMIZATION OF RADIOMETRIC FREQUENCIES

#### 3.1. Optimization with respect to vapor and liquid

The computed brightness temperatures at the mentioned 10 frequencies were used to retrieve the zenith total amount of both water vapor and liquid by the commonly used linear retrieval algorithm which utilizes the zenith optical depth  $\tau$ . The optical depth is obtained from the brightness temperature  $T_{Bi}$  measured at the  $i$ th frequency, the mean radiative temperature at the same frequency  $T_{mi}$ , and the cosmic background  $T_{\text{cos}} = 2.75^\circ\text{K}$ , according to

$$\tau_i = -\ln \left( \frac{T_{mi} - T_{Bi}}{T_{mi} - T_{\text{cos}}} \right). \quad (8)$$

Estimates of the integrated vapor  $\hat{V}$  and liquid  $\hat{L}$  are then linearly related to the  $\tau_i$ s by

$$\hat{V} = a_0 + \sum_{i=1}^{N_f} a_i \tau_i \quad (9)$$

and

$$\hat{L} = b_0 + \sum_{i=1}^{N_f} b_i \tau_i \quad (10)$$

where  $N_f$  is the number of radiometric frequencies and the coefficients  $a_i$  and  $b_i$  are obtained by applying the statistical linear regression analysis to one of the independently generated sets of profiles (training set).

The brightness temperatures relative to the other set of profiles (evaluation set) are used as data in (8); then (9) and (10) give the retrieved  $\hat{V}$  and  $\hat{L}$ . These quantities are finally compared with the corresponding quantities of each profile to obtain the rms retrieval error.

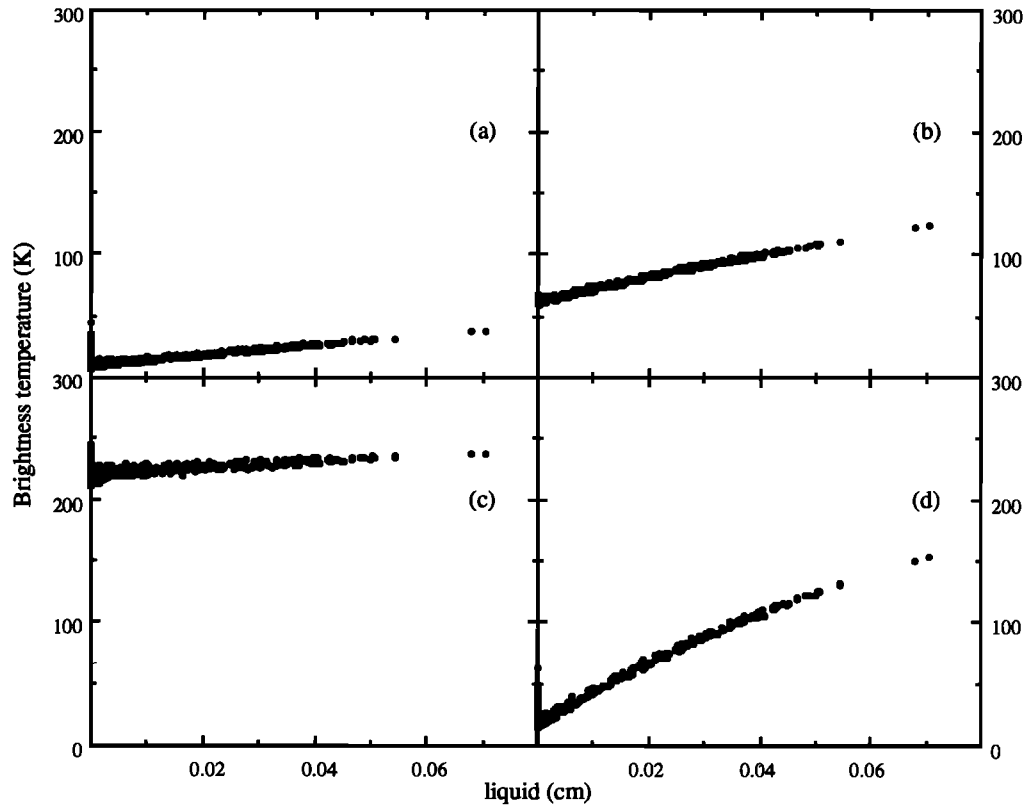


Fig. 2. Brightness temperature for zenith-looking radiometer at (a) 23.9, (b) 0.0, (c) 54.0, and (d) 90.0 GHz for subarctic winter conditions versus water content of clouds.

To simulate noise in the radiometric channels, random fluctuations with Gaussian distribution and varying standard deviations have been added to the brightness temperature data. The results presented

here refer to three levels of rms radiometric noise, that is, 0.5, 1.0, and 2.0 K.

3.1.1. *Mid-latitude summer.* The results of the numerical analysis for mid-latitude summer condi-

TABLE 2a. Rank of Sets of Two Frequencies in Retrieving Vapor and Liquid for Different Standard Deviations of Radiometric Noise, Where Ranking Refers to  $\Delta T = 1$  K and for Mid-Latitude Summer Conditions

Rank	Vapor rms Error, cm					Liquid rms Error, cm				
	$f$ , GHz		Radiometric Noise, K			$f$ , GHz		Radiometric Noise, K		
			0.5	1.0	2.0			0.5	1.0	2.0
1	22.2	36.0	0.098	0.118	0.175	50.0	58.0	0.0061	0.0065	0.0078
2	23.9	36.0	0.073	0.119	0.213	16.0	50.0	0.0055	0.0067	0.0082
3	22.2	31.6	0.098	0.120	0.178	31.6	50.0	0.0056	0.0067	0.0083
4	23.9	31.6	0.069	0.123	0.225	23.9	50.0	0.0064	0.0068	0.0081
5	22.2	50.0	0.127	0.142	0.191	20.6	50.0	0.0064	0.0068	0.0081
6	20.6	36.0	0.088	0.145	0.254	22.2	50.0	0.0065	0.0068	0.0079
7	20.6	31.6	0.085	0.150	0.264	36.0	50.0	0.0059	0.0069	0.0083
8	23.9	50.0	0.125	0.156	0.230	50.0	54.0	0.0069	0.0072	0.0083
9	16.0	22.2	0.109	0.158	0.255	36.0	58.0	0.0084	0.0087	0.0097
10	20.6	50.0	0.140	0.179	0.268	31.6	58.0	0.0089	0.0092	0.0106

TABLE 2b. Rank of Sets of Three Frequencies in Retrieving Vapor and Liquid for Different Standard Deviations of Radiometric Noise, Where Ranking Refers to  $\Delta T = 1$  K and for Mid-Latitude Summer Conditions

Rank	Vapor rms Error, cm						Liquid rms Error, cm					
	$f$ , GHz		Radiometric Noise, K			$f$ , GHz		Radiometric Noise, K				
			0.5	1.0	2.0			0.5	1.0	2.0		
1	22.2	23.9	36.0	0.069	0.097	0.154	50.0	54.0	58.0	0.0053	0.0060	0.0077
2	22.2	23.9	31.6	0.065	0.097	0.159	16.0	50.0	58.0	0.0053	0.0062	0.0078
3	22.2	36.0	54.0	0.078	0.102	0.162	31.6	50.0	58.0	0.0052	0.0063	0.0078
4	22.2	31.6	54.0	0.078	0.104	0.166	20.6	50.0	54.0	0.0052	0.0063	0.0079
5	20.6	22.2	36.0	0.080	0.104	0.159	23.9	50.0	54.0	0.0053	0.0064	0.0080
6	20.6	23.9	36.0	0.068	0.105	0.183	22.2	50.0	54.0	0.0056	0.0064	0.0079
7	23.9	36.0	54.0	0.064	0.106	0.194	36.0	50.0	58.0	0.0053	0.0064	0.0078
8	20.6	22.2	31.6	0.076	0.106	0.168	23.9	50.0	58.0	0.0061	0.0065	0.0077
9	20.6	23.9	31.6	0.064	0.109	0.195	16.0	20.6	50.0	0.0055	0.0065	0.0081
10	22.2	31.6	58.0	0.090	0.111	0.168	22.2	50.0	58.0	0.0061	0.0065	0.0077

tions are reported in Table 2, which shows the relative ranking of the combinations of two and three frequencies for vapor and liquid retrieval, together with the retrieval accuracies for the three levels of radiometric noise. Note that the ranking is relative to a radiometric noise of 1 K rms.

On the basis of the present simulation for a mid-latitude summer atmosphere, the best pairs of frequencies for vapor retrieval appear to include one frequency on the water absorption line and one in the 31–36 GHz window, that is, the frequencies that are presently employed in dual-channel radiometry [Askne and Westwater, 1986], while the best pairs for liquid retrieval include at least one frequency in the neighborhood of the oxygen absorption complex. Increasing the number of radiometric channels improves the accuracy of retrievals, especially for vapor. The best sets of three frequencies

are still different for vapor and liquid, but the relative differences of retrieval accuracy between the first and the tenth set of frequencies is reduced from 52% to 14% for vapor and from 42% to 8% for liquid.

As indicated by the accuracies attainable by the sets appearing in high-ranking positions, a system having more than two channels, with frequencies in the water vapor line region, the 30–40 GHz window, and the oxygen absorption region, may be a reasonable compromise. It should be also noted that the 90-GHz channel seems to be too largely affected by cloud liquid to be efficiently employed in locations with climatologies similar to the one assumed in this simulation.

3.1.2. *Subarctic winter.* The results of the numerical analysis for subarctic winter conditions are reported in Table 3, which shows the relative rank-

TABLE 3a. Rank of Sets of Two Frequencies in Retrieving Vapor and Liquid for Different Standard Deviations of Radiometric Noise, Where Ranking Refers to  $\Delta T = 1$  K and for Subarctic Winter Conditions

Rank	Vapor rms Error, cm					Liquid rms Error, cm				
	$f$ , GHz		Radiometric Noise, K			$f$ , GHz		Radiometric Noise, K		
			0.5	1.0	2.0			0.5	1.0	2.0
1	22.2	50.0	0.027	0.047	0.088	22.2	90.0	0.0005	0.0007	0.0011
2	22.2	36.0	0.029	0.050	0.094	23.9	90.0	0.0007	0.0009	0.0015
3	22.2	90.0	0.034	0.052	0.095	20.6	90.0	0.0007	0.0010	0.0016
4	22.2	31.6	0.030	0.053	0.098	50.0	90.0	0.0009	0.0011	0.0015
5	23.9	50.0	0.044	0.082	0.148	54.0	90.0	0.0009	0.0011	0.0014
6	16.0	22.2	0.048	0.087	0.145	36.0	50.0	0.0009	0.0011	0.0018
7	23.9	36.0	0.048	0.092	0.169	58.0	90.0	0.0011	0.0012	0.0014
8	22.2	23.9	0.059	0.099	0.160	31.6	50.0	0.0010	0.0012	0.0019
9	23.9	90.0	0.064	0.100	0.171	50.0	54.0	0.0009	0.0013	0.0021
10	23.9	31.6	0.052	0.101	0.179	50.0	58.0	0.0010	0.0013	0.0021

TABLE 3b. Rank of Sets of Three Frequencies in Retrieving Vapor and Liquid for Different Standard Deviations of Radiometric Noise, Where Ranking Refers to  $\Delta T = 1$  K and for Subarctic Winter Conditions

Rank	Vapor rms Error, cm						Liquid rms Error, cm					
	$f$ , GHz		Radiometric Noise, K			$f$ , GHz		Radiometric Noise, K				
			0.5	1.0	2.0			0.5	1.0	2.0		
1	22.2	23.9	50.0	0.024	0.043	0.081	22.2	36.0	90.0	0.0004	0.0006	0.0010
2	20.6	22.2	50.0	0.025	0.044	0.084	22.2	50.0	90.0	0.0004	0.0006	0.0010
3	22.2	50.0	54.0	0.027	0.045	0.082	22.2	31.6	90.0	0.0004	0.0006	0.0011
4	22.2	50.0	58.0	0.027	0.046	0.083	16.0	22.2	90.0	0.0005	0.0007	0.0011
5	22.2	36.0	50.0	0.027	0.047	0.087	22.2	58.0	90.0	0.0005	0.0007	0.0011
6	22.2	50.0	90.0	0.027	0.047	0.087	22.2	54.0	90.0	0.0005	0.0007	0.0011
7	22.2	31.6	50.0	0.027	0.047	0.087	20.6	22.2	90.0	0.0005	0.0007	0.0011
8	16.0	22.2	50.0	0.027	0.047	0.088	22.2	23.9	90.0	0.0005	0.0007	0.0011
9	22.2	54.0	90.0	0.030	0.048	0.084	23.9	50.0	90.0	0.0005	0.0007	0.0012
10	22.2	36.0	54.0	0.028	0.048	0.087	23.9	36.0	90.0	0.0004	0.0008	0.0013

ing of the combinations of two and three frequencies for vapor and liquid retrieval, together with the retrieval accuracies for the three levels of radiometric noise. As before, the ranking is relative to a radiometric noise of 1 K rms.

The most striking difference with respect to the results obtained for the mid-latitude summer case is now the presence of the 90-GHz radiometric channel in the highest ranked sets of frequencies for the retrieval of liquid and, to some extent, of vapor too. This is related to the scarce amount of liquid water in the subarctic winter atmosphere which prevents the 90-GHz channel from saturating, as is shown by a comparison of Figures 1 and 2. Also, the relatively low amount of vapor makes the center frequency of the water vapor line to appear more frequently in the high ranks, due to its generally higher signal-to-noise ratio.

### 3.2. Optimization with respect to attenuation and wet path delay

The previous results indicate that the optimal sets of frequencies for atmospheric vapor retrieval are in general different from the optimal ones for liquid retrieval. For a given temperature and pressure background, space-Earth attenuation in atmospheric windows is a function of both vapor and liquid, whose relative influence depends on frequency. Therefore we expect that the optimal selection of channels for a radiometer dedicated to telecommunication applications may differ from the one obtained previously and may eventually depend on the satellite beacon frequency. On the other hand, a radiometer employed for correcting tropospheric electrical path delays

should have an optimal configuration substantially similar to that for vapor retrieval.

To determine the optimal channel configuration of radiometers for satellite communication and space geodesy applications, the numerical simulation has been used to analyze the effects of different selections of the number of channels and of radiometric frequencies on the accuracy of prediction of zenith attenuation  $A$  and wet path delay  $D$ . To this end, three linear statistical retrieval approaches can be followed: in the first,  $A$  and  $D$  are related to the brightness temperatures; in the second,  $A$  and  $D$  are related to the optical depths, while in the third,  $A$  and  $D$  are related to  $\hat{V}$  and  $\hat{L}$  obtained from the  $T_{Bs}$ , as outlined in section 3.1. The results that will be discussed here have been obtained by the second approach, which, according to our simulations, yields the highest retrieval accuracy. The already cited MPM has been used to evaluate  $A$  and  $D$  at selected beacon frequencies for each synthetic atmosphere of the training set; then  $A$  and  $D$  have been statistically related to the optical depths  $\tau$  evaluated from the  $T_{Bs}$  of the same training set for different combinations of the radiometric frequencies. In turn, the  $\tau$ s have been used to estimate  $A$  and  $D$  at the beacon frequencies for each individual profile of the evaluation set. Finally, the combinations of radiometric frequencies have been ranked in order of decreasing accuracy in attenuation and wet delay predictions.

3.2.1. *Mid-latitude summer.* The above mentioned procedure has been followed to analyze the performance of the various combinations of two and three frequencies for the mid-latitude summer

TABLE 4a. Rank of Sets of Two Frequencies in Retrieving Attenuation and Wet Path Delay at 40 GHz for Different Standard Deviations of Radiometric Noise, Where Ranking Refers to  $\Delta T = 1$  K and for Mid-Latitude Summer Conditions

Rank	Attenuation rms Error, dB					Path Delay rms Error, cm				
	$f$ , GHz		Radiometric Noise, K			$f$ , GHz		Radiometric Noise, K		
			0.5	1.0	2.0			0.5	1.0	2.0
1	31.6	54.0	0.032	0.044	0.074	22.2	36.0	0.60	0.71	1.07
2	36.0	54.0	0.037	0.045	0.067	22.2	31.6	0.58	0.73	1.09
3	22.2	31.6	0.036	0.047	0.074	23.9	36.0	0.47	0.75	1.33
4	20.6	31.6	0.036	0.047	0.076	23.9	31.6	0.44	0.76	1.38
5	23.9	31.6	0.035	0.048	0.077	22.2	50.0	0.77	0.87	1.15
6	22.2	36.0	0.042	0.049	0.069	20.6	36.0	0.57	0.88	1.55
7	23.9	36.0	0.041	0.049	0.070	20.6	31.6	0.54	0.90	1.62
8	20.6	36.0	0.042	0.049	0.069	16.0	22.2	0.64	0.93	1.52
9	31.6	36.0	0.048	0.050	0.063	23.9	50.0	0.81	0.98	1.45
10	36.0	58.0	0.045	0.051	0.071	20.6	50.0	0.90	1.11	1.66

atmosphere. Tables 4–6 report the relative ranking of sets of two and three frequencies with respect to the accuracy of prediction of zenith attenuation and wet path delay at three different frequencies, that is, 40, 50, and 90 GHz for the usual three levels of radiometric noise. Again, ranking is given with respect to a radiometric resolution of 1 K.

The best pairs of radiometric frequencies vary with the particular frequency at which attenuation is to be estimated, while they remain almost unchanged for path delay, which is essentially independent of frequency. The optimal pairs of frequencies for attenuation, which depends on both vapor and liquid, in general are not optimal for time delay, which depends essentially on vapor only, although at 40 and 50 GHz, a dual-channel radiometer with 22.2 and 31.6 or 36.0 GHz appears to perform well with respect to both  $A$  and  $D$ . As for vapor and liquid, increasing the number of channels from two

to three leads to an improvement in accuracy, which is more appreciable for path delay than for attenuation. The results reported in Tables 4–6 do not define uniquely a basic radiometric configuration performing equally well for both attenuation and path delay at all frequencies. However, as in the case of  $V$  and  $L$ , an instrument with at least three radiometric channels with frequencies on the water vapor line, in an atmospheric window, and in the region of oxygen absorption, respectively, seems to be reasonable.

Finally, it should be pointed out that the inclusion of meteorological data at ground level into the retrieval scheme yielded only a moderate improvement in the performance of a dual-channel radiometer. The improvement is lower than the one attainable by the addition of an appropriate third radiometric channel. The result obtained for the synthetic atmospheres has

TABLE 4b. Rank of Sets of Three Frequencies in Retrieving Attenuation and Wet Path Delay at 40 GHz for Different Standard Deviations of Radiometric Noise, Where Ranking Refers to  $\Delta T = 1$  K and for Mid-Latitude Summer Conditions

Rank	Attenuation rms Error, dB						Path Delay rms Error, cm					
	$f$ , GHz			Radiometric Noise, K			$f$ , GHz			Radiometric Noise, K		
				0.5	1.0	2.0				0.5	1.0	2.0
1	31.6	36.0	54.0	0.032	0.039	0.055	22.2	23.9	36.0	0.44	0.58	0.92
2	23.9	31.6	36.0	0.035	0.041	0.058	22.2	23.9	31.6	0.41	0.60	0.98
3	16.0	31.6	54.0	0.030	0.042	0.071	22.2	36.0	54.0	0.46	0.62	0.96
4	22.2	31.6	36.0	0.036	0.043	0.057	22.2	31.6	54.0	0.46	0.62	1.00
5	20.6	31.6	36.0	0.036	0.043	0.059	20.6	22.2	31.6	0.47	0.64	0.99
6	16.0	36.0	54.0	0.033	0.043	0.064	20.6	22.2	36.0	0.49	0.65	0.97
7	31.6	54.0	58.0	0.031	0.044	0.074	23.9	36.0	54.0	0.42	0.65	1.18
8	36.0	50.0	54.0	0.028	0.044	0.065	20.6	23.9	36.0	0.44	0.66	1.14
9	16.0	22.2	31.6	0.033	0.044	0.072	20.6	23.9	31.6	0.40	0.67	1.20
10	20.6	31.6	54.0	0.032	0.044	0.073	22.2	36.0	58.0	0.58	0.69	1.01

TABLE 5a. Rank of Sets of Two Frequencies in Retrieving Attenuation and Wet Path Delay at 50 GHz for Different Standard Deviations of Radiometric Noise, Where Ranking Refers to  $\Delta T = 1$  K and for Mid-Latitude Summer Conditions

Rank	Attenuation rms Error, dB					Path Delay rms Error, cm				
	$f$ , GHz		Radiometric Noise, K			$f$ , GHz		Radiometric Noise, K		
			0.5	1.0	2.0			0.5	1.0	2.0
1	22.2	36.0	0.041	0.055	0.094	22.2	36.0	0.59	0.71	1.05
2	36.0	54.0	0.038	0.055	0.095	22.2	31.6	0.58	0.73	1.08
3	23.9	36.0	0.040	0.057	0.098	23.9	36.0	0.47	0.74	1.31
4	20.6	36.0	0.042	0.058	0.096	23.9	31.6	0.44	0.76	1.37
5	22.2	31.6	0.037	0.059	0.111	22.2	50.0	0.78	0.87	1.15
6	31.6	54.0	0.039	0.062	0.112	20.6	36.0	0.57	0.90	1.55
7	23.9	31.6	0.036	0.062	0.114	20.6	31.6	0.54	0.92	1.60
8	20.6	31.6	0.038	0.063	0.115	16.0	22.2	0.65	0.94	1.50
9	36.0	58.0	0.056	0.066	0.098	23.9	50.0	0.81	0.99	1.42
10	31.6	58.0	0.056	0.072	0.112	20.6	50.0	0.89	1.13	1.61

been confirmed for sets of actual radiosonde-measured profiles over various locations in Italy.

It should also be noted that the highest-ranked sets of frequencies for attenuation at 50 and 90 GHz do not include these frequencies. Indeed, our simulation indicated that, for mid-latitude summer conditions, radiometric frequencies coincident with the ones of the beacon generally yield the highest accuracy in attenuation prediction only in the ideal case, that is, for a noiseless instrument and when the mean radiating temperature is exactly known.

3.2.2. *Subarctic winter.* The results of the numerical analysis for subarctic winter conditions are reported in Tables 7–9, which show the relative ranking of sets of two and three frequencies with respect to the accuracy of prediction of zenith attenuation and wet path delay at three different frequencies, that is, 40, 50, and 90 GHz for the usual three levels of

radiometric noise. Again, ranking is given with respect to a radiometric resolution of 1 K.

As seen before for vapor and liquid retrieval, a major difference with respect to the results obtained for the mid-latitude summer case is now the presence of the 90-GHz radiometric channel in several high-ranking sets of frequencies for the prediction of both attenuation and wet path delay at all the considered frequencies. In particular, the 90-GHz channel appears in all the first nine 2- and 3-channel configurations for attenuation prediction at 90 GHz, unlike in the mid-latitude summer case. Indeed, the subarctic winter atmosphere contains a scarce amount of liquid water, so that radiometric saturation at 90 GHz, which substantially reduces its retrieval potential, seldom occurs. As far as a basic radiometric configuration is concerned, an instrument with at least three channels with frequencies on the water vapor

TABLE 5b. Rank of Sets of Three Frequencies in Retrieving Attenuation and Wet Path Delay at 50 GHz for Different Standard Deviations of Radiometric Noise, Where Ranking Refers to  $\Delta T = 1$  K and for Mid-Latitude Summer Conditions

Rank	Attenuation rms Error, dB						Path Delay rms Error, cm					
	$f$ , GHz			Radiometric Noise, K			$f$ , GHz			Radiometric Noise, K		
				0.5	1.0	2.0				0.5	1.0	2.0
1	22.2	31.6	36.0	0.033	0.045	0.075	22.2	23.9	36.0	0.44	0.60	0.92
2	23.9	31.6	36.0	0.033	0.047	0.078	22.2	23.9	31.6	0.41	0.60	0.95
3	31.6	36.0	54.0	0.034	0.048	0.079	22.2	36.0	54.0	0.46	0.62	0.97
4	20.6	31.6	36.0	0.034	0.049	0.080	22.2	31.6	54.0	0.46	0.62	1.00
5	22.2	36.0	54.0	0.037	0.052	0.091	20.6	22.2	36.0	0.50	0.64	0.95
6	16.0	22.2	36.0	0.036	0.054	0.090	20.6	22.2	31.6	0.47	0.64	1.01
7	16.0	36.0	54.0	0.036	0.054	0.093	20.6	23.9	36.0	0.44	0.64	1.13
8	20.6	36.0	54.0	0.038	0.054	0.094	23.9	36.0	54.0	0.42	0.66	1.19
9	23.9	36.0	54.0	0.038	0.055	0.095	20.6	23.9	31.6	0.41	0.68	1.21
10	16.0	23.9	36.0	0.035	0.055	0.095	22.2	36.0	58.0	0.57	0.69	1.02

TABLE 6a. Rank of Sets of Two Frequencies in Retrieving Attenuation and Wet Path Delay at 90 GHz for Different Standard Deviations of Radiometric Noise, Where Ranking Refers to  $\Delta T = 1$  K and for Mid-Latitude Summer Conditions

Rank	Attenuation rms Error, dB					Path Delay rms Error, cm				
	$f$ , GHz		Radiometric Noise, K			$f$ , GHz		Radiometric Noise, K		
			0.5	1.0	2.0			0.5	1.0	2.0
1	36.0	50.0	0.12	0.14	0.19	22.2	31.6	0.59	0.72	1.10
2	50.0	54.0	0.10	0.14	0.23	22.2	36.0	0.60	0.72	1.07
3	22.2	50.0	0.11	0.14	0.23	23.9	36.0	0.48	0.75	1.32
4	23.9	50.0	0.11	0.14	0.23	23.9	31.6	0.44	0.76	1.38
5	31.6	50.0	0.12	0.14	0.20	22.2	50.0	0.77	0.86	1.14
6	20.6	50.0	0.11	0.14	0.22	20.6	36.0	0.57	0.90	1.55
7	16.0	50.0	0.12	0.15	0.23	20.6	31.6	0.54	0.93	1.62
8	50.0	58.0	0.12	0.15	0.24	16.0	22.2	0.64	0.93	1.52
9	36.0	54.0	0.17	0.19	0.26	23.9	50.0	0.80	0.98	1.42
10	20.6	36.0	0.17	0.19	0.26	20.6	50.0	0.90	1.11	1.64

line, around 50 GHz, and at 90 GHz seems a reasonable choice for this kind of climatic conditions.

#### 4. SUMMARY AND CONCLUSIONS

A number of scientists now apply microwave radiometry, and several international programs are underway for deployment of microwave radiometers. A variety of applications is envisaged, including meteorology, satellite communication studies, and space geodesy. For this reason, establishing some basic design specifications of a multipurpose instrument could be advisable, especially from the point of view of cost reduction.

Through a numerical simulation, we analyzed the predicted performance of a ground-based radiometer in retrieving atmospheric moisture content and in estimating Earth-space attenuation and path de-

lay at several frequencies in the millimeter-wave range. Sets of atmospheric realizations have been statistically generated from mid-latitude summer and subarctic winter standard atmospheres, including humidity and temperature irregularities, ground-based inversions, liquid clouds and/or fog. These sets of profiles can be made representative of particular locations within the respective climatologies by adjusting the relevant generating parameters. The synthetic realizations of the atmospheric profiles have been used to obtain the brightness temperatures as would be measured by a microwave radiometer aiming at zenith. Ten radiometric frequencies in the range 16–90 GHz have been selected and the possible combinations of two or more synthetic measurements have been used to retrieve integrated vapor and liquid. To simulate noise in the radiometric channels, random fluctuations with

TABLE 6b. Rank of Sets of Three Frequencies in Retrieving Attenuation and Wet Path Delay at 90 GHz for Different Standard Deviations of Radiometric Noise, Where Ranking Refers to  $\Delta T = 1$  K and for Mid-Latitude Summer Conditions

Rank	Attenuation rms Error, cm						Path Delay rms Error, cm					
	$f$ , GHz			Radiometric Noise, K			$f$ , GHz			Radiometric Noise, K		
				0.5	1.0	2.0				0.5	1.0	2.0
1	36.0	50.0	54.0	0.10	0.12	0.18	22.2	23.9	36.0	0.44	0.60	0.93
2	31.6	50.0	54.0	0.10	0.13	0.19	22.2	23.9	31.6	0.41	0.60	0.97
3	20.6	36.0	50.0	0.11	0.13	0.18	22.2	36.0	54.0	0.46	0.61	0.97
4	22.2	36.0	50.0	0.11	0.13	0.18	22.2	31.6	54.0	0.46	0.62	1.01
5	23.9	36.0	50.0	0.11	0.13	0.18	20.6	22.2	36.0	0.50	0.64	0.98
6	23.9	31.6	50.0	0.11	0.13	0.19	20.6	22.2	31.6	0.47	0.65	1.02
7	20.6	31.6	50.0	0.11	0.13	0.19	20.6	23.9	36.0	0.45	0.66	1.13
8	20.6	50.0	58.0	0.11	0.13	0.22	23.9	36.0	54.0	0.41	0.67	1.18
9	50.0	54.0	58.0	0.10	0.14	0.23	20.6	23.9	31.6	0.40	0.67	1.21
10	16.0	50.0	54.0	0.10	0.14	0.22	22.2	36.0	58.0	0.57	0.69	1.01

TABLE 7a. Rank of Sets of Two Frequencies in Retrieving Attenuation and Wet Path Delay at 40 GHz for Different Standard Deviations of Radiometric Noise, Where Ranking Refers to  $\Delta T = 1$  K and for Subarctic Winter Conditions

Rank	Attenuation rms Error, dB					Path Delay rms Error, cm				
	$f$ , GHz		Radiometric Noise, K			$f$ , GHz		Radiometric Noise, K		
			0.5	1.0	2.0			0.5	1.0	2.0
1	36.0	50.0	0.009	0.015	0.027	22.2	50.0	0.19	0.32	0.59
2	31.6	50.0	0.009	0.015	0.028	22.2	36.0	0.21	0.35	0.64
3	50.0	90.0	0.012	0.016	0.025	22.2	90.0	0.24	0.36	0.65
4	50.0	54.0	0.012	0.018	0.034	22.2	31.6	0.21	0.36	0.67
5	23.9	50.0	0.012	0.018	0.033	23.9	50.0	0.30	0.55	0.99
6	20.6	50.0	0.012	0.018	0.033	16.0	22.2	0.33	0.59	0.98
7	22.2	50.0	0.012	0.019	0.034	23.9	36.0	0.33	0.62	1.12
8	50.0	58.0	0.012	0.020	0.034	23.9	31.6	0.36	0.66	1.18
9	16.0	50.0	0.013	0.020	0.034	22.2	23.9	0.40	0.67	1.09
10	54.0	90.0	0.019	0.021	0.027	23.9	90.0	0.43	0.69	1.16

varying standard deviations have been added to the brightness temperature data. The retrieved  $V$  and  $L$  have then been compared with the corresponding quantities of each profile to obtain the rms retrieval error. Since a major goal of the study was the performance analysis of a radiometer for propagation parameter estimation, a study of the accuracy in predicting both attenuation and wet path delay for a vertical Earth-space path has been performed.

Some conclusions can be drawn from the analysis.

1. The optimal sets of frequencies determined for mid-latitude summer conditions differ from those appropriate for subarctic winter. The main source of discrepancy resides in the saturation of the 90-GHz channel by the relatively abundant liquid water present in mid-latitude summer clouds. This result indicates that each climatic condition may require a different optimal radiometric configuration (region-

specific instrument). Similarly, the retrieval coefficients may depend on the local climatology.

2. As a general feature, an optimal basic configuration of a multichannel radiometer appears to require the presence of at least one channel around the water vapor line, at least one channel in a window region, and at least one channel in the oxygen complex frequency region. If the instrument is mainly intended for optimal operation in subarctic winter conditions, a channel in the 70- to 100-GHz window region (e.g., 90 GHz) is appropriate. For mid-latitude climates, this frequency range is of limited use because of saturation.

3. The analysis described here has been extended to four and five channels, with the indication that the performance enhancement is generally reduced if the number of channels exceeds three. Therefore the increase in cost of the instrument is

TABLE 7b. Rank of Sets of Three Frequencies in Retrieving Attenuation and Wet Path Delay at 40 GHz for Different Standard Deviations of Radiometric Noise, Where Ranking Refers to  $\Delta T = 1$  K and for Subarctic Winter Conditions

Rank	Attenuation rms Error, dB						Path Delay rms Error, cm					
	$f$ , GHz			Radiometric Noise, K			$f$ , GHz			Radiometric Noise, K		
				0.5	1.0	2.0				0.5	1.0	2.0
1	31.6	36.0	50.0	0.008	0.014	0.025	22.2	23.9	50.0	0.16	0.29	0.53
2	36.0	50.0	90.0	0.009	0.014	0.023	20.6	22.2	50.0	0.17	0.30	0.55
3	22.2	36.0	50.0	0.009	0.014	0.027	22.2	50.0	54.0	0.18	0.30	0.54
4	16.0	36.0	50.0	0.009	0.014	0.027	22.2	50.0	58.0	0.18	0.31	0.55
5	20.6	36.0	50.0	0.009	0.015	0.027	22.2	50.0	90.0	0.18	0.32	0.59
6	23.9	36.0	50.0	0.009	0.015	0.027	22.2	31.6	50.0	0.18	0.32	0.59
7	36.0	50.0	58.0	0.009	0.015	0.027	22.2	54.0	90.0	0.20	0.32	0.57
8	31.6	50.0	90.0	0.009	0.015	0.024	16.0	22.2	50.0	0.18	0.32	0.59
9	36.0	50.0	54.0	0.009	0.015	0.027	22.2	36.0	54.0	0.19	0.32	0.58
10	16.0	31.6	50.0	0.009	0.015	0.028	22.2	36.0	50.0	0.18	0.32	0.59

TABLE 8a. Rank of Sets of Two Frequencies in Retrieving Attenuation and Wet Path Delay at 50 GHz for Different Standard Deviations of Radiometric Noise, Where Ranking Refers to  $\Delta T = 1$  K and for Subarctic Winter Conditions

Rank	Attenuation rms Error, dB					Path Delay rms Error, cm				
	$f$ , GHz	Radiometric Noise, K			$f$ , GHz	Radiometric Noise, K				
		0.5	1.0	2.0		0.5	1.0	2.0		
1	50.0	54.0	0.016	0.028	0.053	22.2	50.0	0.18	0.32	0.59
2	50.0	58.0	0.023	0.031	0.052	22.2	36.0	0.20	0.34	0.63
3	22.2	50.0	0.023	0.032	0.054	22.2	90.0	0.24	0.36	0.63
4	23.9	50.0	0.024	0.033	0.057	22.2	31.6	0.21	0.36	0.65
5	54.0	90.0	0.028	0.034	0.052	23.9	50.0	0.29	0.54	0.99
6	20.6	50.0	0.024	0.035	0.058	16.0	22.2	0.33	0.58	0.98
7	50.0	90.0	0.021	0.039	0.063	23.9	36.0	0.33	0.62	1.13
8	36.0	54.0	0.022	0.040	0.074	23.9	90.0	0.42	0.67	1.14
9	31.6	50.0	0.031	0.045	0.064	23.9	31.6	0.35	0.68	1.18
10	36.0	50.0	0.032	0.046	0.062	22.2	23.9	0.40	0.68	1.07

TABLE 8b. Rank of Sets of Three Frequencies in Retrieving Attenuation and Wet Path Delay at 50 GHz for Different Standard Deviations of Radiometric Noise, Where Ranking Refers to  $\Delta T = 1$  K and for Subarctic Winter Conditions

Rank	Attenuation rms Error, dB						Path Delay rms Error, cm					
	$f$ , GHz	Radiometric Noise, K			$f$ , GHz	Radiometric Noise, K						
		0.5	1.0	2.0		0.5	1.0	2.0				
1	36.0	50.0	54.0	0.015	0.024	0.046	22.2	23.9	50.0	0.16	0.28	0.54
2	31.6	50.0	54.0	0.015	0.025	0.047	20.6	22.2	50.0	0.17	0.29	0.56
3	50.0	54.0	90.0	0.016	0.025	0.042	22.2	50.0	54.0	0.18	0.31	0.54
4	20.6	50.0	54.0	0.016	0.027	0.052	22.2	50.0	58.0	0.18	0.31	0.55
5	23.9	50.0	54.0	0.015	0.027	0.052	22.2	36.0	50.0	0.18	0.31	0.59
6	16.0	50.0	54.0	0.016	0.027	0.053	22.2	31.6	50.0	0.18	0.31	0.59
7	22.2	50.0	54.0	0.016	0.027	0.053	16.0	22.2	50.0	0.18	0.31	0.59
8	50.0	54.0	58.0	0.016	0.028	0.051	22.2	36.0	54.0	0.19	0.32	0.59
9	36.0	54.0	90.0	0.020	0.030	0.048	22.2	54.0	90.0	0.21	0.32	0.56
10	36.0	50.0	58.0	0.022	0.030	0.048	22.2	50.0	90.0	0.17	0.32	0.59

TABLE 9a. Rank of Sets of Two Frequencies in Retrieving Attenuation and Wet Path Delay at 90 GHz for Different Standard Deviations of Radiometric Noise, Where Ranking Refers to  $\Delta T = 1$  K and for Subarctic Winter Conditions

Rank	Attenuation rms Error, dB					Path Delay rms Error, cm				
	$f$ , GHz	Radiometric Noise, K			$f$ , GHz	Radiometric Noise, K				
		0.5	1.0	2.0		0.5	1.0	2.0		
1	36.0	90.0	0.014	0.024	0.043	22.2	50.0	0.18	0.31	0.60
2	50.0	90.0	0.016	0.024	0.042	22.2	36.0	0.21	0.35	0.64
3	31.6	90.0	0.016	0.026	0.045	22.2	90.0	0.24	0.36	0.65
4	54.0	90.0	0.020	0.028	0.046	22.2	31.6	0.21	0.36	0.66
5	22.2	90.0	0.021	0.028	0.046	23.9	50.0	0.29	0.55	0.99
6	58.0	90.0	0.021	0.028	0.045	16.0	22.2	0.32	0.59	0.99
7	20.6	90.0	0.022	0.029	0.048	23.9	36.0	0.33	0.62	1.13
8	23.9	90.0	0.022	0.029	0.049	23.9	31.6	0.36	0.67	1.21
9	16.0	90.0	0.023	0.030	0.048	22.2	23.9	0.40	0.68	1.09
10	50.0	54.0	0.032	0.054	0.102	23.9	90.0	0.44	0.69	1.15

TABLE 9b. Rank of Sets of Three Frequencies in Retrieving Attenuation and Wet Path Delay at 90 GHz for Different Standard Deviations of Radiometric Noise, Where Ranking Refers to  $\Delta T = 1$  K and for Subarctic Winter Conditions

Rank	Attenuation rms Error, dB						Path Delay rms Error, cm					
	$f$ , GHz			Radiometric Noise, K			$f$ , GHz			Radiometric Noise, K		
				0.5	1.0	2.0				0.5	1.0	2.0
1	36.0	50.0	90.0	0.014	0.022	0.040	22.2	23.9	50.0	0.17	0.29	0.54
2	31.6	50.0	90.0	0.014	0.022	0.040	22.2	50.0	54.0	0.18	0.30	0.55
3	31.6	36.0	90.0	0.013	0.022	0.041	20.6	22.2	50.0	0.17	0.30	0.57
4	20.6	50.0	90.0	0.015	0.022	0.040	16.0	22.2	50.0	0.18	0.31	0.59
5	23.9	50.0	90.0	0.015	0.023	0.039	22.2	50.0	58.0	0.19	0.31	0.56
6	22.2	50.0	90.0	0.016	0.023	0.042	22.2	50.0	90.0	0.18	0.31	0.60
7	50.0	54.0	90.0	0.014	0.023	0.041	22.2	54.0	90.0	0.21	0.32	0.55
8	16.0	50.0	90.0	0.016	0.023	0.041	22.2	31.6	50.0	0.18	0.32	0.60
9	16.0	36.0	90.0	0.014	0.023	0.043	22.2	36.0	50.0	0.19	0.32	0.59
10	23.9	36.0	90.0	0.014	0.023	0.043	22.2	36.0	54.0	0.19	0.32	0.58

probably not justified by its improvement in performance, at least if the linear statistical inversion is employed. Further study is needed to ascertain how a profiling inversion scheme [Robinson, 1988] could more effectively use the additional pieces of information provided by the additional channels.

**Acknowledgments.** This work has been carried out within a contract from European Space Agency (ESA), monitored by J. P. V. Poyares Baptista (The primary contractor is SMA, Florence). The authors wish to thank B. Arbesser-Rastburg, G. Brussaard, and J. P. V. Poyares Baptista for stimulating discussion and suggestions. The authors also acknowledge the valuable suggestions made by J. Schroeder on the manuscript. Radiosonde data have been provided by the Meteorological Service of the Italian Air Force.

#### REFERENCES

- Askne, J. I. H., and E. R. Westwater, A review of ground-based remote sensing of temperature and moisture by passive microwave radiometers, *IEEE Trans. Geosci. Remote Sens.*, *GE-24*, 340–352, 1986.
- Brussaard, G., Radiometry, *Eur. Space Agency Spec. Publ.*, *ESA SP-1071*, 120 pp., 1985.
- Decker, M. T., E. R. Westwater, and F. O. Guiraud, Experimental evaluation of ground-based microwave radiometric sensing of atmospheric temperature and water vapor profiles, *J. Appl. Meteorol.*, *17*, 1788–1795, 1978.
- Elgered, G., B. O. Rönnäng, and J. I. H. Askne, Measurement of atmospheric water vapor with microwave radiometry, *Radio Sci.*, *17*, 1258–1264, 1982.
- Elgered, G., J. Davis, T. A. Herring, and I. I. Shapiro, Geodesy by radio interferometry: Water vapor radiometry for estimation of the wet delay, *J. Geophys. Res.*, *96*(B4), 6541–6555, 1991.
- Gary, B. L., S. J. Keihm, and M. A. Janssen, Optimum strategies and performance for the remote sensing of path-delay using ground-based microwave radiometers, *IEEE Trans. Geosci. Remote Sens.*, *GE-23*, 479–484, 1985.
- Grody, N. C., Remote sensing of atmospheric water content from satellites using microwave radiometry, *IEEE Trans. Antennas Propag.*, *AP-24*(2), 155–162, 1976.
- Hogg, D. C., F. O. Guiraud, J. B. Snider, M. T. Decker, and E. R. Westwater, A steerable dual-channel microwave radiometer for measurements of water vapor and liquid in the troposphere, *J. Appl. Meteorol.*, *22*, 789–806, 1983.
- Liebe, H. S., MPM—An atmospheric millimeter-wave propagation model *Int. J. Infrared Millimeter Waves*, *10*, 631–650, 1989.
- McClatchey, R. A., and A. P. D'Agati, Atmospheric transmission of laser radiation: computer code LASER, *Environ. Res. Pap.* 622, (AFGL-TR-78-0029), 138 pp., 1978.
- Robinson, S. E., The profile algorithm for microwave delay estimation from water vapor radiometer data, *Radio Sci.*, *23*, 401–408, 1988.
- Snider, J. B., Verification of the accuracy of a network of water-vapour radiometers, Proceedings of the IGARSS '88 Symposium, *Eur. Space Agency Spec. Publ.*, *ESA SP-284*, 19–20, 1988.
- Soong, T. T., *Probabilistic Modeling and Analysis in Science and Engineering*, pp. 206–209, John Wiley, New York, 1982.
- Ware, R. H., C. Rocken, and J. B. Snider, Experimental verification of improved GPS-measured baseline repeatability using water-proof radiometer corrections, *IEEE Trans. Geosci. Remote Sens.*, *GE-23*, 467–473, 1985.
- Westwater, E. R., and F. O. Guiraud, Ground-based microwave radiometric retrieval of precipitable water vapor in the presence of clouds with high liquid content, *Radio Sci.*, *15*, 947–957, 1980.
- Westwater, E. R., and O. N. Strand, Statistical information content of radiation measurements used in indirect sensing, *J. Atmos. Sci.*, *25*, 750–758, 1968.
- Westwater, E. R., J. B. Snider, and M. J. Falls, Ground-based radiometric observation of atmospheric emission and attenuation at 20.6, 31.65, and 90.0 GHz: A comparison of measurements and theory, *IEEE Trans. Antennas Propag.*, *AP-38*(10), 1569–1580, 1990.
- G. Schiavon and D. Solimini, Dipartimento di Ingegneria Elettronica, Università Tor Vergata, Via O. Raimondo, 00173 Roma, Italy.
- E. R. Westwater, NOAA/ERL Wave Propagation Laboratory, Boulder, CO 80309.